

Electronic Supplementary Information

Design and Characterization of Alkoxy-wrapped Push-pull Porphyrins for Dye-sensitized Solar Cells

Teresa Ripolles-Sanchis,^a Bo-Cheng Guo,^b Hui-Ping Wu,^c Tsung-Yu Pan,^c Hsuan-Wei Lee,^b Sonia R. Raga,^a Francisco Fabregat-Santiago,^a Juan Bisquert,^{*a} Chen-Yu Yeh,^{*b} and Eric Wei-Guang Diau^{*c}

^a *Photovoltaics and Optoelectronic Devices Group, Departament de Física, Universitat Jaume I, 12071 Castelló, Spain. Tel: +34-964-38-7540; E-mail: bisquert@fca.uji.es*

^b *Department of Chemistry and Center of Nanoscience & Nanotechnology, National Chung Hsing University, Taichung 402, Taiwan. Fax: +886-4-22862547; Tel: +886-4-22852264; Email: cyyeh@dragon.nchu.edu.tw*

^c *Department of Applied Chemistry and Institute of Molecular Science, National Chiao Tung University, Hsinchu 30010, Taiwan. Fax: +886-3-5723764; Tel: +886-3-5131524; E-mail: diau@mail.nctu.edu.tw*

Optical and Electrochemical Properties in Solution

The UV-Visible absorption spectra of **YD20**, **YD21** and **YD22** in THF at 23 °C are shown in Figure S1. The maximum peaks of the absorption spectra and the molar absorption coefficients of the Soret and Q absorption bands under the same conditions are summarized in Table S1.

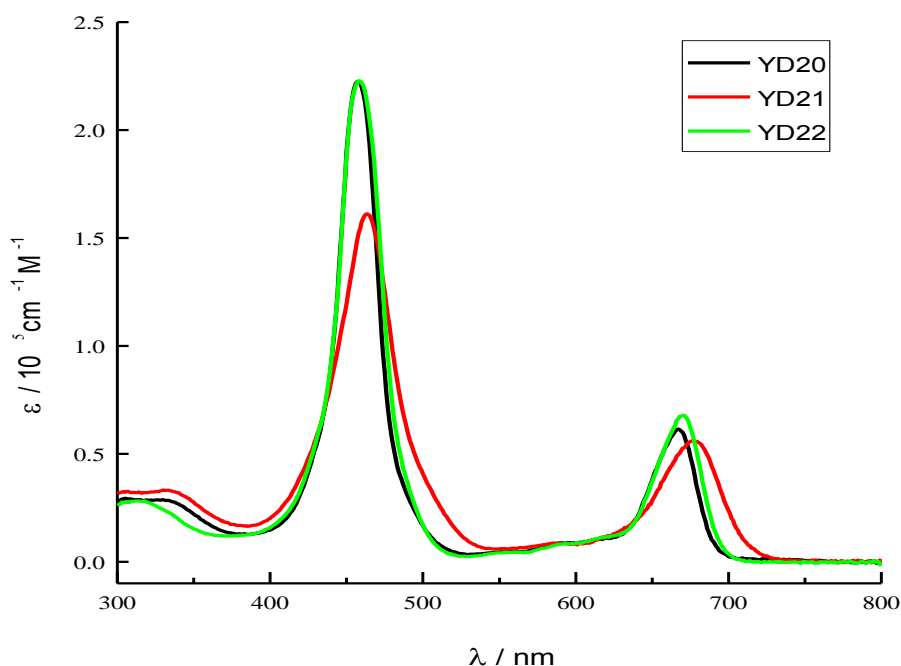


Figure S1. The UV/Vis absorption spectra of porphyrin dyes **YD20** (black), **YD21** (red), and **YD22** (green) in THF at 23 °C.

Porphyrins typically show in the absorption spectra a maximum attributed to π - π^* transitions in the range 400-450 nm for an intense Soret absorption band and 500-700 nm for the moderate Q absorption bands. The molar absorption coefficients ($10^3 \text{ M}^{-1} \text{ cm}^{-1}$) for the Soret band of **YD20**, **YD21**, and **YD22** are 223, 172, and 223, respectively; in respect to the Q bands, the molar absorption coefficients ($10^3 \text{ M}^{-1} \text{ cm}^{-1}$) are 61, 56, and 68 for **YD20**, **YD21**, and **YD22**, respectively.

YD20 and **YD22** dyes have virtually the same intense Soret band (at 457 nm and 459 nm, respectively) and a low intense Q band (at 667 nm and 671 nm, respectively). The

molar absorption coefficients for **YD20** and **YD22** dyes are equal ($223 \cdot 10^3 \text{ M}^{-1} \text{ cm}^{-1}$) for the Soret band and similar values for the Q band ($61 \cdot 10^3 \text{ M}^{-1} \text{ cm}^{-1}$ and $68 \cdot 10^3 \text{ M}^{-1} \text{ cm}^{-1}$, respectively). These results are due to the fact that both porphyrin-dyes have the same acceptor group, an acid group which will attach itself into the TiO_2 nanoparticles.

The Soret band for **YD21** dye has low intensity absorption at 463 nm and the Q band for **YD21** dye is slightly red-shifted (677 nm) with respect to the other porphyrin sensitizers, **YD20** (667 nm) and **YD22** (671 nm) dyes. The slightly red-shifted Q band for **YD21** dye results are due to an elongation of the π -conjugation and loss of symmetry in the porphyrin structure which is caused by the cyanoacrylic acid. Also, the **YD21** dye has the lowest molar absorption coefficient for the Soret and Q bands ($172 \cdot 10^3 \text{ M}^{-1} \text{ cm}^{-1}$ and $56 \cdot 10^3 \text{ M}^{-1} \text{ cm}^{-1}$) compared with **YD20** and **YD22** dyes.

The emission data was measured in THF and the wavelengths for emission maxima are shown in Table 1. Similar to the UV-Vis absorption spectra results, the emission is red-shifted (703 nm) on the incorporation of a cyanoacrylic acid for the **YD21** with respect to the acid group for the **YD20** (674 nm) and **YD22** (676 nm) dyes.

Table S1. Spectral and electrochemical data for porphyrin dyes.^a

Dye	Absorption	Emission ^b	Oxidation	Reduction
	$\lambda_{\text{max}}/\text{nm}$ ($\epsilon/10^3 \text{ M}^{-1} \text{ cm}^{-1}$)	λ_{max} (nm) (ϕ)	$E_{1/2}$ (V)	$E_{1/2}$ (V)
YD20	457(223), 667(61)	674	+0.84, +1.03	-1.19
YD21	463(172), 677(56)	703	+0.85, +1.03	-1.18
YD22	459(223), 671(68)	676	+0.78, +1.02	-1.21

^a Absorption and emission data were measured in THF at 23°C. Electrochemical measurements were performed at 23°C in THF containing TBAPF_6 (0.1 M) as supporting electrolyte. Potentials measured vs. ferrocene/ferrocenium (Fc/Fc^+) couple were converted to a normal hydrogen electrode (NHE) by the addition of +0.63 V.

^b The excitation wavelengths were 450 nm in THF.

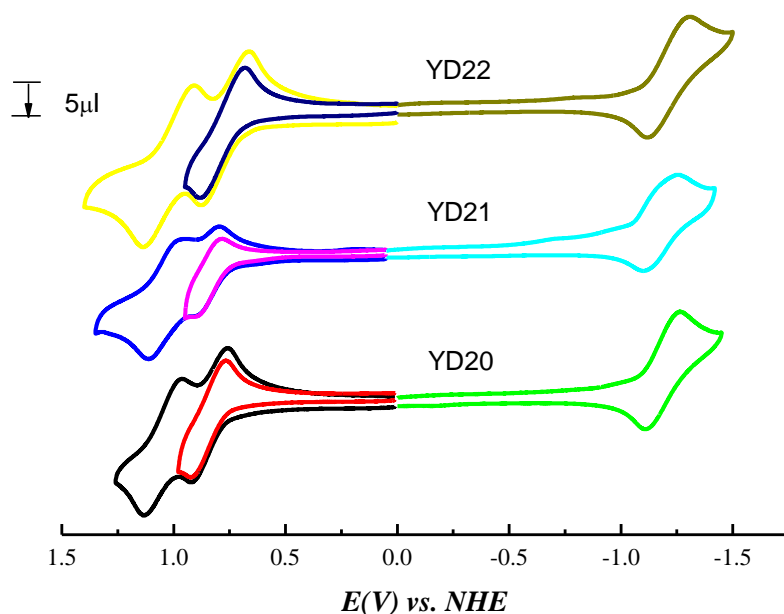


Figure S2. Cyclic voltammograms of **YD20-YD22** dyes.

The redox potential of these porphyrins in solution was measured by using cyclic voltammetry, which shows well-resolved and reversible electron waves (Figure S2). The oxidation and reduction potentials of these sensitizers are listed in Table S1. These three porphyrin dyes show similar electrochemical behavior with two oxidation and one reduction waves in solution. The oxidation corresponds to the highest occupied molecular orbital (HOMO) energy of the dye which has to be more positive than the redox couple I/I_3^- energy for a good regeneration yield of the dye (Figure S3). These three porphyrin dyes have the same behavior, such as two different oxidations peaks and one reduction peak. The two oxidations correspond to electron abstractions from both the amino functional group and the porphyrin ring.

The highest occupied molecular orbital-lowest unoccupied molecular orbital (HOMO-LUMO) data are summarized in the energy diagram for **YD20-YD22** dyes are detailed in the support information in Figure 3. There is a correlation between band gap data with the UV-Vis absorption and emission data. **YD20** and **YD22** dyes have the same absorption and similar band gap, 1.85 V and 1.84 V, respectively. In contrast, **YD21** dye has the absorption spectra are red-shifted because the lowest band gap energy compared with **YD20** and **YD22** dyes.

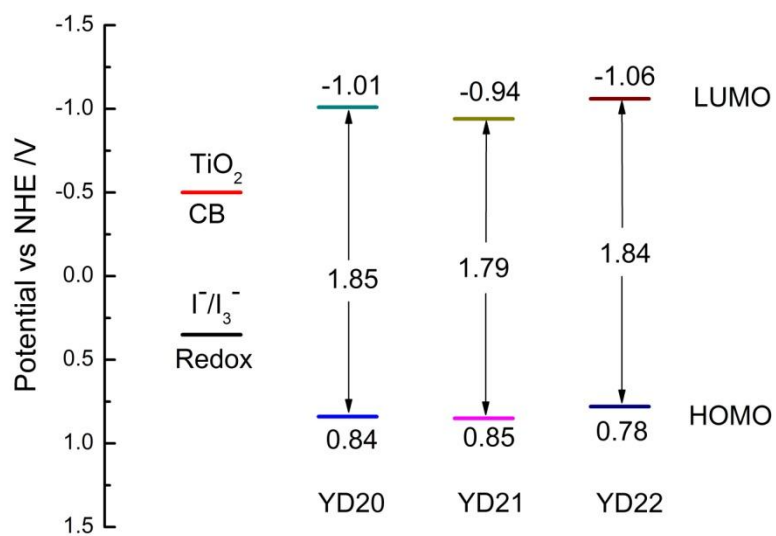


Figure S3. A schematic energy-level diagram of porphyrins **YD20-YD22**.

Experimental Section

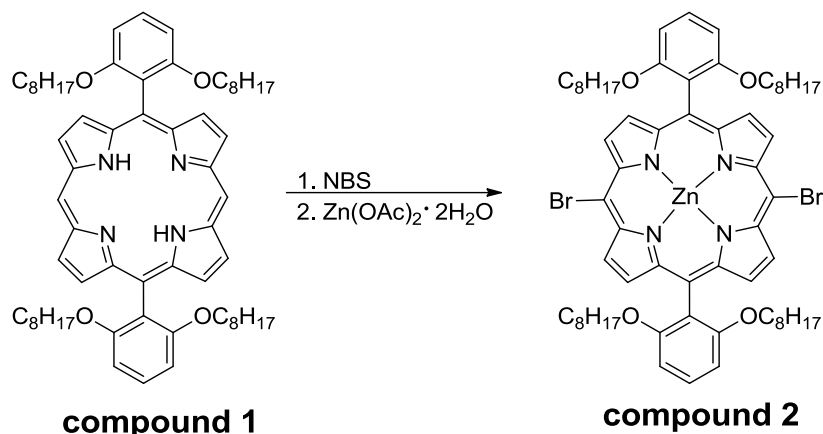
General

All reagents and solvents were obtained from commercial sources and used without further purification unless otherwise noted. THF was dried over sodium/ benzophenone and freshly distilled before use. Tetra-*n*-butylammonium hexafluorophosphate (TBAPF₆) was recrystallized twice from absolute ethanol and further dried for two days under vacuum. Column chromatography was performed on silica gel (Merck, 70-230 Mesh ASTM).

Spectral and electrochemical measurements

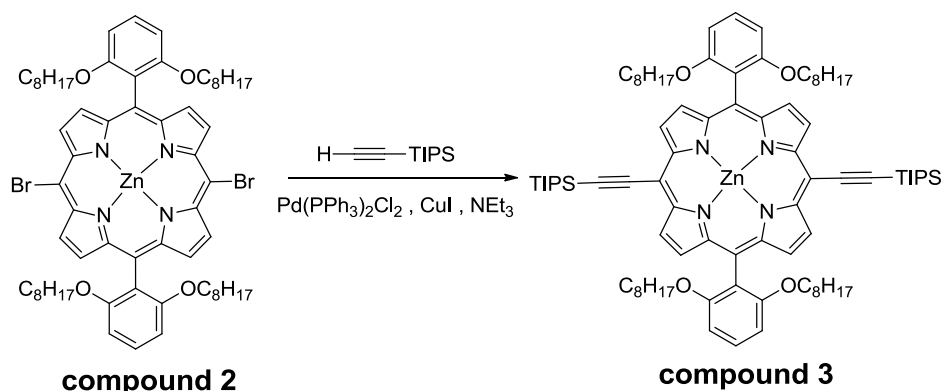
¹H and ¹³C NMR spectra were recorded on a Varian 400 MHz. Chemical shifts for ¹H NMR spectra are referenced in the deuterated solvent (CHCl₃ δ = 7.26 ppm for ¹H and δ = 77 ppm for ¹³C). Spectra were recorded at room temperature, chemical shifts are written in ppm and coupling constants in Hz. UV-visible spectra (Varian Cary 50), emission spectra (a JASCO FP-6000 spectrofluorometer), ESI-MS mass spectra (Finnigan TSQ Ultra EMR, Tandem Mass spectrometer, operating in the positive ion detection mode) was recorded on the indicated instrument. Electrochemistry was performed with a three-electrode potentiostat (CH Instruments, Model 750A) in THF deoxygenated by purging with prepurified N₂ gas. Cyclic voltammetry was conducted with the use of a home-made three-electrode cell equipped with a BAS glassy carbon (0.07 cm²) disk as the working electrode, a platinum wire as the auxiliary electrode, and a home-made Ag/AgCl (saturated) reference electrode. The reference electrode is separated from the bulk solution by a double junction filled with electrolyte solution. Potentials are reported vs Ag/AgCl (saturated) and referenced to the ferrocene/ferrocenium (Fc/Fc⁺) couple which occurs at $E_{1/2} = +0.63$ V vs Ag/AgCl (saturated). The working electrode was polished with 0.03 μm alumina on Buehler felt pads and washed with deionized water prior to each experiment. The reproducibility of individual potential values was within ±5 mV.

Synthesis of compound 2:



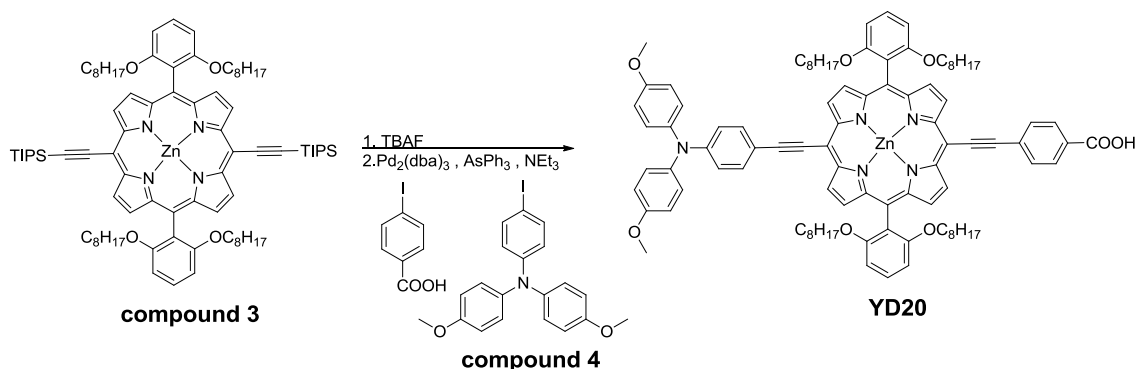
In a round-bottom flask **compound 1**¹ (2.0 g, 2.05 mmol) and anhydrous dichloromethane (1500 mL) were stirred. Then a solution of N-bromosuccinimide (0.73 g, 4.1 mmol) in dichloromethane (250 mL) was slowly added under nitrogen flow. After 2 hours, a solution of acetone (50 mL) was quickly added. Stirring was maintained for 30 min. The solution was passed a short column and then Zn(OAc)₂ · 2H₂O (2.25 g, 10.3 mmol) were added. The solution was stirred at room temperature for 24 hours and then water was added. The mixture was extracted with dichloromethane and the organic layer was collected. The solvent was removed under vacuum and the residue was purified by column chromatography (silica gel) using dichloromethane/hexane (1/1) as eluent. Recrystallization from dichloromethane/methanol to get **compound 2** (2.23 g, 91%). ¹H NMR (400 MHz, CDCl₃) δ 9.64 (d, *J* = 4.2 Hz, 4H), 8.90 (d, *J* = 4.2 Hz, 4H), 7.71 (t, *J* = 7.8 Hz, 2H), 7.01 (d, *J* = 7.8 Hz, 4H), 3.85 (t, *J* = 5.4 Hz, 8H), 1.02 – 0.91 (m, 8H), 0.88 – 0.75 (m, 8H), 0.66 – 0.57 (m, 8H), 0.57 – 0.42 (m, 28H), 0.42 – 0.32 (m, 8H). ¹³C NMR (101 MHz, CDCl₃) δ 159.9, 151.4, 149.7, 132.8, 130.0, 120.7, 114.9, 105.1, 103.9, 68.6, 31.4, 28.6, 25.3, 22.3, 13.8. ESI: m/z: Calcd for C₆₄H₈₂Br₂N₄O₄Zn: 1197 [M+H]⁺, Found: 1196.4 [M+H]⁺

Synthesis of compound 3:



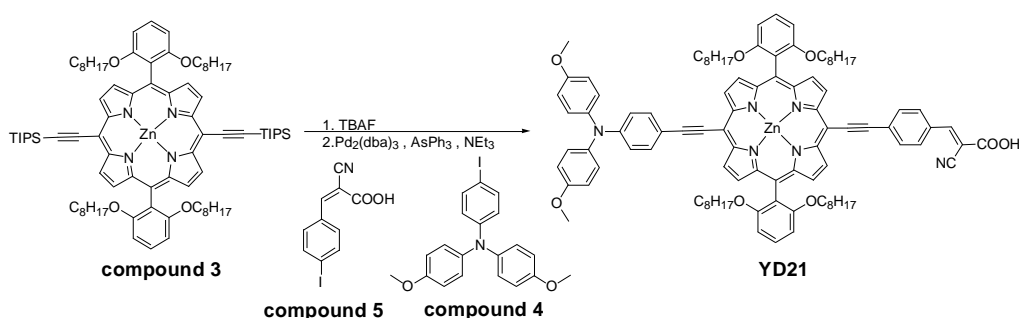
In a round-bottom flask **compound 2** (2.0 g, 2.05 mmol) and anhydrous THF (45 mL) and (triisopropylsilyl)acetylene (0.75 ml, 3.34 mmol) and copper(I) iodide (31.8 mg, 0.167mmol) were stirred under nitrogen atmosphere. Triethylamine (12 mL) was then added and the mixture was degassed by N₂ bubbling. Pd(PPh₃)₂Cl₂ (117 mg, 0.167mmol) was added and the solution was heated at 85 °C overnight. The solvent was removed under vacuum and the residue was purified by column chromatography (silica gel) using dichloromethane/hexane (1/3) as eluent. Solvent were removed to afford **compound 3** (1637 mg, 70%) as purple solid. ¹H NMR (400 MHz, CDCl₃) δ 9.69 (d, *J* = 4.4 Hz, 4H), 8.89 (d, *J* = 4.4 Hz, 4H), 7.68 (t, *J* = 8.4 Hz, 2H), 6.99 (d, *J* = 8.4 Hz, 4H), 3.83 (t, *J* = 6.4 Hz, 8H), 1.55 – 1.45 (m, 42H), 1.00 – 0.91 (m, 8H), 0.80 – 0.70 (m, 8H), 0.58 – 0.51 (m, 8H), 0.51 – 0.45 (m, 28H), 0.44 – 0.33 (m, 8H). ¹³C NMR (101 MHz, CDCl₃) δ 159.9, 152.0, 150.6, 131.7, 130.8, 129.7, 121.1, 114.9, 110.1, 105.4, 100.2, 96.5, 68.8, 31.3, 28.5, 25.2, 22.2, 19.1, 13.8, 11.9. ESI: *m/z*: Calcd for C₈₆H₁₂₄N₄O₄Si₂Zn: 1399 [M+H]⁺, Found: 1398.9 [M+H]⁺

Synthesis of YD20:



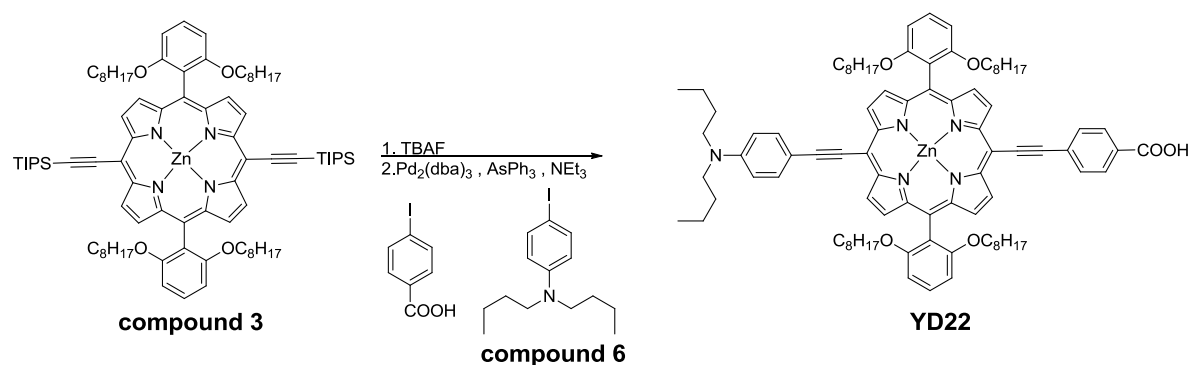
To a solution of **compound 3** (100 mg, 0.071 mmol) in (5 mL) was added tetra-*n*-butylammonium fluoride (0.715 mL, 0.71 mmol) at room temperature. Before water was added, the mixture was stirred for 1 hr. The solution was extracted with dichloromethane, the green organic layer was collected, and the solvent was evaporated under reduced pressure to get the deprotected intermediate. To a solution of the deprotected intermediate in a degassed mixture of THF (20 mL) and NEt₃ (3 mL) was added 4-iodobenzoic acid (21.8 mg, 0.085 mmol), and **compound 4**² (37 mg, 0.085 mmol), Pd₂(dba)₃ (3.25 mg, 3.55 μmol), and AsPh₃ (43 mg, 0.142 mmol). The mixture was stirred at 85 °C for 5 hours. The solvent was removed under vacuum and the residue was purified by column chromatography (silica gel) using CH₂Cl₂/CH₃OH (19/1) as eluent. Recrystallization from CH₂Cl₂/CH₃OH gave **YD20** (37 mg, 34%). ¹H NMR (400 MHz, CDCl₃/CD₃OD) δ 9.59 (dd, *J* = 7.5, 4.5 Hz, 4H), 8.81 (d, *J* = 4.5 Hz, 2H), 8.77 (d, *J* = 4.5 Hz, 2H), 8.19 (d, *J* = 8.2 Hz, 2H), 8.03 (d, *J* = 8.2 Hz, 2H), 7.77 (d, *J* = 8.8 Hz, 2H), 7.69 (t, *J* = 8.4 Hz, 2H), 7.16 (d, *J* = 9.0 Hz, 4H), 7.05 (d, *J* = 8.8 Hz, 2H), 7.01 (d, *J* = 8.4 Hz, 4H), 6.89 (d, *J* = 9.0 Hz, 4H), 3.86 (t, *J* = 6.5 Hz, 8H), 3.82 (s, 6H), 1.01 – 0.92 (m, 8H), 0.92 – 0.84 (m, 8H), 0.75 – 0.67 (m, 8H), 0.61 – 0.54 (m, 28H), 0.50 – 0.40 (m, 8H). ¹³C NMR (101 MHz, CDCl₃/CD₃OD) δ 159.8, 156.1, 151.7, 151.3, 150.4, 150.3, 148.6, 140.4, 132.3, 130.5, 130.1, 129.6, 127.0, 121.2, 119.7, 115.5, 114.8, 105.3, 101.5, 97.3, 94.6, 92.3, 68.7, 31.4, 29.7, 28.7, 28.6, 28.5, 25.2, 22.3, 13.9. ESI: *m/z*: Calcd for C₉₅H₁₀₅N₅O₈Zn: 1510 [M+H]⁺, Found: 1509.9 [M+H]⁺

Synthesis of YD21:



A procedure similar to **YD20** was employed for the synthesis of **YD21** (31%). ¹H NMR (400 MHz, CDCl₃/CD₃OD) δ 9.57 (dd, *J* = 7.5, 4.5 Hz, 4H), 8.77 (d, *J* = 4.5 Hz, 2H), 8.73 (d, *J* = 4.5 Hz, 2H), 8.26 (s, 1H), 8.13 (d, *J* = 8.2 Hz, 2H), 8.03 (d, *J* = 8.2 Hz, 2H), 7.75 (d, *J* = 8.6 Hz, 2H), 7.66 (t, *J* = 8.4 Hz, 2H), 7.15 (d, *J* = 8.9 Hz, 4H), 7.03 (d, *J* = 8.6 Hz, 2H), 6.98 (d, *J* = 8.4 Hz, 4H), 6.88 (d, *J* = 8.9 Hz, 4H), 3.86 – 3.80 (m, 14H), 0.99 – 0.90 (m, 8H), 0.89 – 0.84 (m, 8H), 0.76 – 0.66 (m, 8H), 0.61 – 0.52 (m, 28H), 0.49 – 0.41 (m, 8H). ¹³C NMR (101 MHz, CDCl₃/CD₃OD) δ 159.7, 156.2, 151.8, 151.3, 150.4, 150.2, 148.6, 140.4, 132.3, 131.8, 131.5, 131.2, 130.8, 130.4, 130.1, 129.6, 128.8, 128.5, 127.0, 121.0, 119.7, 119.0, 115.5, 114.8, 105.1, 68.6, 31.4, 28.7, 28.6, 28.5, 25.2, 22.3, 13.8. ESI: *m/z*: Calcd for C₉₈H₁₀₆N₆O₈Zn: 1561 [M+H]⁺, Found: 1560.9 [M+H]⁺

Synthetic of YD22:



A procedure similar to **YD20** was employed for the synthesis of **YD22** (32%). ¹H NMR (400 MHz, CDCl₃/CD₃OD) δ 9.61 (d, *J* = 4.5 Hz, 2H), 9.58 (d, *J* = 4.5 Hz, 2H), 8.79 (d,

$J = 4.5$ Hz, 2H), 8.74 (d, $J = 4.5$ Hz, 2H), 8.20 (d, $J = 8.2$ Hz, 2H), 8.02 (d, $J = 8.2$ Hz, 2H), 7.82 (d, $J = 9.0$ Hz, 2H), 7.69 (t, $J = 8.4$ Hz, 2H), 7.01 (d, $J = 8.4$ Hz, 4H), 6.77 (d, $J = 9.0$ Hz, 2H), 3.85 (t, $J = 6.4$ Hz, 8H), 3.38 (t, $J = 8$ Hz, 4H), 1.70 – 1.62 (m, 4H), 1.46 – 1.39 (m, 4H), 1.01 – 0.95 (m, 14H), 0.92 – 0.85 (m, 8H), 0.77 – 0.68 (m, 8H), 0.64 – 0.55 (m, 28H), 0.51 – 0.45 (m, 8H). ^{13}C NMR (101 MHz, $\text{CDCl}_3/\text{CD}_3\text{OD}$) δ 159.8, 151.3, 150.3, 150.1, 147.9, 132.9, 131.8, 131.1, 131.0, 130.6, 130.0, 129.6, 121.2, 114.7, 111.4, 110.1, 105.3, 97.3, 94.6, 91.1, 68.7, 31.4, 29.7, 29.4, 28.7, 28.6, 28.5, 25.2, 22.3, 20.4, 14.0, 13.9. ESI: m/z : Calcd for $\text{C}_{89}\text{H}_{109}\text{N}_5\text{O}_6\text{Zn}$: 1410 $[\text{M}+\text{H}]^+$, Found: 1409.9 $[\text{M}+\text{H}]^+$

Device fabrication and characterization

The porphyrin-sensitized solar-cell (PSSC) devices were fabricated with a working electrode based on TiO_2 nanoparticles (NP) and a Pt-coated counter electrode. For the working electrode, a paste composed of TiO_2 NP (particle size ~ 25 nm) prepared with a sol-gel method for the transparent nanocrystalline layer was coated on a TiCl_4 -treated FTO glass substrate (TEC 7, Hartford) to obtain the required thickness (~ 15 μm) on repetitive screen printing. To improve the performance of the PSSC, an additional scattering layer (particle size ~ 300 nm) was screen-printed on the transparent active layer. The electrode was then immersed in a dye solution (0.2 mM) with EtOH/Toluene = 1/1 at 25 $^\circ\text{C}$ for 3 h for dye loading onto the TiO_2 film. The dye-sensitized electrode was rinsed with ethanol and dried by an air-gun. The Pt counter electrodes were prepared on spin-coating drops of H_2PtCl_6 solution onto FTO glass and heating at 385 $^\circ\text{C}$ for 15 min. The porphyrin working electrode and the thermally platinized counter electrode were separated and sealed with a hot-melt film (Surlyn, Dupont, thickness 60 μm). The internal space was filled with a volatile electrolyte, which is a composition of 0.6 M propylmethylimidazolium iodide (PMII), 50 mM I_2 , 10 mM LiI, 0.1 M Guanidinium thiocyanate (GuNCS), 0.5 M tert-butylpyridine (TBP) and a mixture of solvents acetonitrile:valeronitrile (85:15 vol). The performance of a PSSC device was assessed through measurement of a $J-V$ curve with an AM-1.5 G solar simulator (XES-502S, SAN-EI), calibrated with a Si-based reference cell (S1133, Hamamatsu). The incident monochromatic efficiencies for conversion from photons to current (IPCE) spectra of the corresponding devices were measured with a system comprising a Xe lamp (PTi A-1010, 150 W), monochromator (PTi, 1200 gr mm^{-1} blazed at 500 nm), and source meter (Keithley 2400, computer controlled). A standard Si photodiode (S1337-1012BQ, Hamamatsu) served as a reference to calibrate the power density of the light source at each wavelength.

Electrochemical Impedance Spectroscopy (EIS) measurements

Acquisition of the EIS measurements were carried out with a Zahner impedance analyzer controlled from a computer with Thales software. The amplitude of the AC signal was 20 mV and its frequency ranged between 1 MHz and 10 mHz. Bias potentials used were comprised between 0 and 0.75 V. Illumination in impedance spectroscopy measurements was provided by a LED source. The power of the LED lamp was adjusted to obtain the same V_{OC} as in J - V curves taken under illumination with a solar simulator at 1 sun irradiation (AM1.5G, 100 mW cm⁻²).

Reference:

- 1) Yella, A.; Lee, H.W.; Tsao, H. N.; Yi, C.; Chandiran, A. K.; Nazeeruddin, M. K.; Diau, E.W. G.; Yeh, C. Y.; Zakeeruddin, S. M.; Grätzel, M. *Science* **2011**, *334*, 629.
- 2) Lin, J.-H.; Elangovan, A.; Ho, T.-I. *J. Org. Chem.* **2005**, *70*, 7397-7407
- 3) Lee, C. Y.; She, C.; Jeong, N. C.; Hupp, J. T. *Chem. Commun.* **2010**, *46*, 6090-6092.